

# Cluster model of decagonal tilings

Michael Reichert<sup>1,2,\*</sup> and Franz Gähler<sup>1</sup>

<sup>1</sup>*Institut für Theoretische und Angewandte Physik, Universität Stuttgart,  
D-70550 Stuttgart, Germany*

<sup>2</sup>*Fachbereich Physik, Universität Konstanz, D-78457 Konstanz, Germany*  
(Dated: November 11, 2018)

A relaxed version of Gummelt's covering rules for the aperiodic decagon is considered, which produces certain random-tiling-type structures. These structures are precisely characterized, along with their relationships to various other random tiling ensembles. The relaxed covering rule has a natural realization in terms of a vertex cluster in the Penrose pentagon tiling. Using Monte Carlo simulations, it is shown that the structures obtained by maximizing the density of this cluster are the same as those produced by the corresponding covering rules. The entropy density of the covering ensemble is determined using the entropic sampling algorithm. If the model is extended by an additional coupling between neighboring clusters, perfectly ordered structures are obtained, like those produced by Gummelt's perfect covering rules.

PACS numbers: 61.44.Br, 64.60.Cn

## I. INTRODUCTION

Many quasicrystals are completely covered by overlapping copies of a single cluster (Fig. 1). Two overlapping clusters must agree in the overlap region, which restricts the possible relative positions and orientations of neighboring clusters. Cluster overlaps therefore create order, in favorable cases even perfect quasiperiodic order.

This observation can be used to formulate several variants of an ordering principle for quasicrystals (for a review, see Ref. 3): A perfect quasicrystal can be obtained by requiring either that a given cluster completely covers the structure, or that the cluster has maximal density in the structure, or that it covers the structure with maximal density. With such ordering principles, perfect quasiperiodic order could be obtained for decagonal,<sup>4,5</sup> octagonal,<sup>6</sup> and dodecagonal<sup>7</sup> tilings and quasicrystals. Assuming that such a cluster is an energetically preferred atomic configuration, the maximization of the cluster density minimizes the free energy. With this hypothesis, the covering approach might serve as a simple thermodynamic mechanism for the formation of quasicrystals. The covering approach can be regarded as a particularly simple realization of energy based matching rules, where only the most important local configurations (the clusters) have to be preferred energetically<sup>8</sup>, not all allowed local configurations. As a variant, it has also been suggested<sup>9</sup> to penalize the worst local configurations, instead of preferring the best ones, which provides another way to simplify the matching rule approach.

The same ordering principles can also be used to produce supertile random tiling structures, which are locally ordered but show disorder on larger scales. These structures are obtained whenever the chosen cluster is not selective enough and hence allows too many different overlaps.<sup>3</sup> This happens, in particular, if the cluster is too small to restrict the number of different overlaps,<sup>10</sup> or if it is too symmetric. In this respect, it is interesting to note that *asymmetric* clusters seem to be preferred

by the electronic structure in decagonal quasicrystals.<sup>11</sup> Whereas supertile random tilings are locally ordered for energetic reasons, their long range order is produced by entropy maximization, as is the case for other random tilings<sup>12</sup>.

In this paper, we will concentrate on cluster models for decagonal structures. Gummelt's aperiodic decagon<sup>4</sup> provides a striking example how perfect quasiperiodic order can be obtained by a simple cluster covering principle. This example has been so convincing, that many researchers tried to map their experimental structures to the Gummelt decagon, even though the fit in the overlap was often not perfect (see, e. g., Refs. 11 and 13), and the overlapping constraints not exactly equivalent. However,

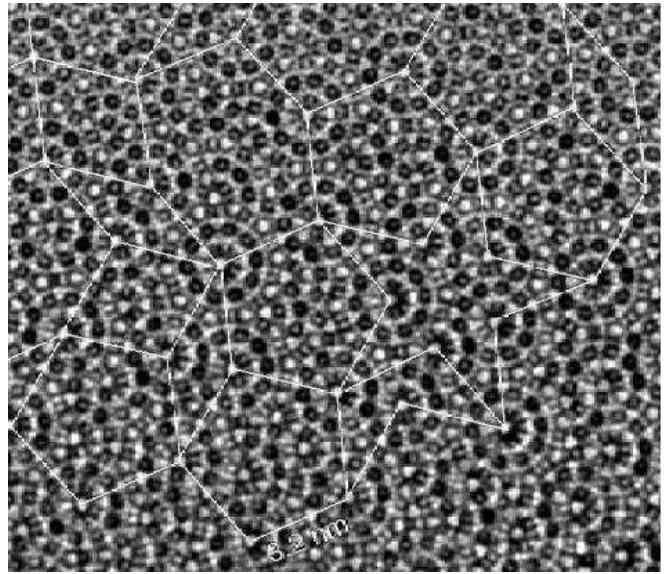


FIG. 1: High-resolution transmission electron microscopy image of decagonal Al-Ni-Co (courtesy of S. Ritsch and C. Beeli, compare Ref. 1). The superimposed tiling has been reconstructed by an automated procedure.<sup>2</sup>

many experimental decagonal quasicrystal structures are not perfectly quasiperiodic, and it is therefore interesting to consider also overlap rules which are less restrictive than the perfect rules of Gummelt, and which do not enforce perfectly ordered, but rather (supertile) random tiling structures.

The analysis of such relaxed overlap rules and their corresponding structures will be the main topic of this paper.<sup>14</sup> In Sec. II, two different relaxed versions of Gummelt's overlap rules are discussed, and the structures which they produce are precisely characterized, along with their relationships to various other random tiling ensembles. Subsequently, in Sec. III we introduce a vertex cluster in the Penrose pentagon tiling (PPT) whose structure imposes the previously discussed overlap constraints in a natural way. It is shown by Monte Carlo (MC) simulations that the structures with maximal density of this cluster are the same as those produced by the corresponding overlap rules. In Sec. IV, we determine the entropy density of the set of states with maximal cluster density, using the entropic sampling algorithm. An additional coupling between neighboring clusters is introduced in Sec. V, and it is shown that this coupling is capable of ordering the random tilings to perfectly ordered structures.

## II. COVERINGS FOR PERFECT AND RANDOM PENROSE PENTAGON TILINGS

It is well known that each covering of the plane by Gummelt's aperiodic decagon (Fig. 2(a)) is equivalent to a perfect Penrose tiling,<sup>4</sup> if the covering has the following property: Whenever two decagons overlap, their colorings agree in the entire overlap region. It turns out that Gummelt's rule permits only two different types of overlaps, which are shown in Fig. 2(b): the smaller A- and the larger B-overlaps. Furthermore, due to the coloring, there are only certain overlap zones for allowed

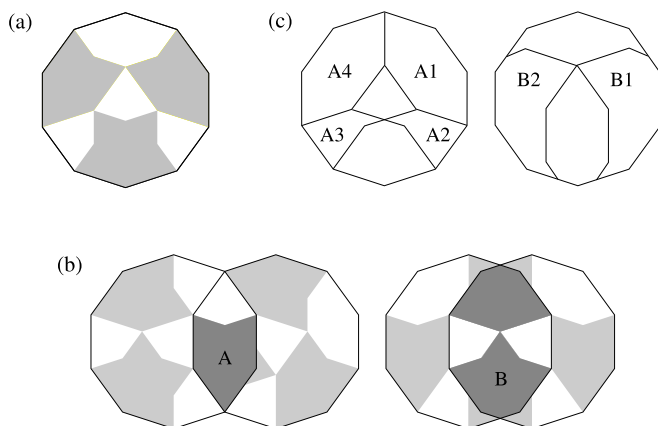


FIG. 2: Gummelt decagon (a), representative A- and B-overlap (b), and allowed overlap zones (c).

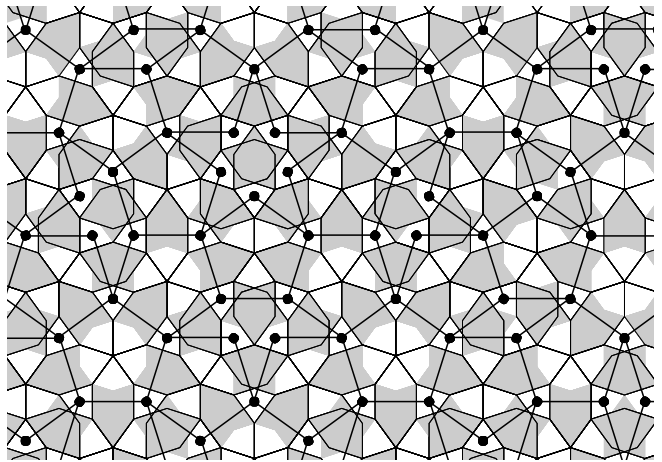


FIG. 3: Perfect PPT, superimposed on the corresponding Gummelt decagon covering.

overlaps with neighboring decagons: four for A- and two for B-overlaps (Fig. 2(c)). This altogether is what we will call the *perfect rule* (in order to distinguish it from other variants being discussed later).

The decagon centers of such a *perfect covering* form the vertex set of a *perfect PPT* (Fig. 3). Conversely, each PPT can be obtained from exactly one covering satisfying the Gummelt overlap rules. We therefore have a local one-to-one correspondence between PPTs and Gummelt coverings. As the Gummelt decagon represents a cluster in the corresponding quasicrystal, we will often use the term cluster for the covering decagon.

In order to allow for partially disordered coverings, Gummelt et al.<sup>15,16</sup> have proposed to relax the overlap rules to some extent. To understand the type of relaxation, recall that if the perfect rules are obeyed, a decagon may have small A-overlaps with neighboring decagons in four possible directions, and bigger B-overlaps with neighboring decagons in two possible directions (Fig. 2(c)). The coloring in the overlap region has an orientation, which must be respected. All possible overlaps are therefore *oriented*. As a relaxation of the perfect rule, Gummelt et al.<sup>15,16</sup> have proposed to abandon this orientation constraint, and to retain only the *non-oriented overlap zones*, as shown in Fig. 2(c). This overlap rule will be referred to as the fully relaxed rule.

There is a natural intermediate rule between the perfect and the fully relaxed rule. In this variant, which will be called the *relaxed rule*, the orientation condition is abandoned only for the small A-overlaps, but is retained for the larger B-overlaps. This kind of overlap rule can be motivated physically as follows: The large B-overlaps result in a strong interaction between the two overlapping clusters, which must be in its ground state, whereas the small A-overlaps only lead to a weak interaction with a small energy difference between differently oriented A-overlaps. This intermediate rule and the resulting structures will be the main topic of this paper.

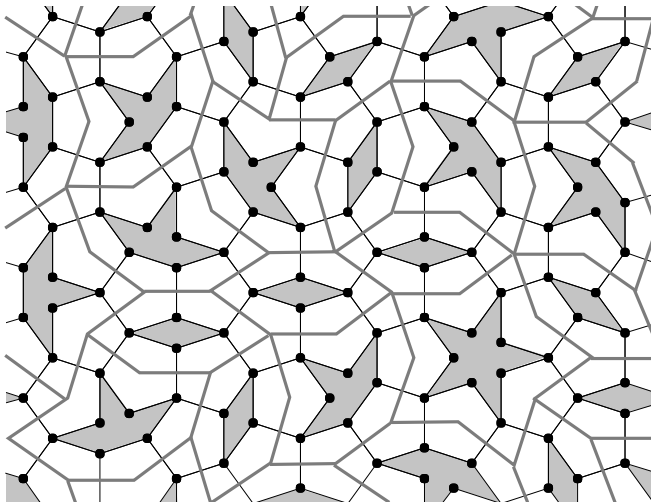


FIG. 4: Random PPT with all the spiky tiles (shaded in gray) surrounded by pentagons. This tiling is equivalent to a random HBS tiling (gray lines), whose tile edges connect the centers of neighboring pentagons.

Gummelt et al.<sup>15,16</sup> have shown that each covering satisfying the fully relaxed rule has the property that its cluster centers form the vertex set of a random PPT. It has the additional property that all the spiky tiles (stars, ships, and rhombi; shaded in gray in Fig. 4) are completely surrounded by pentagons. (In the following, when we use the term “random PPT”, we always mean one satisfying this extra condition; more general ones do not play any role here.) Such a random PPT is equivalent to a random hexagon-boat-star (HBS) tiling (gray lines in Fig. 4). Since coverings satisfying the more restrictive relaxed rule also satisfy the fully relaxed rule, their cluster centers form the vertex set of a random PPT, too. Conversely, it is easy to see that every random PPT can arise both from relaxed and from fully relaxed coverings. The only difference between relaxed and fully relaxed coverings is the number of coverings associated with a given random PPT.

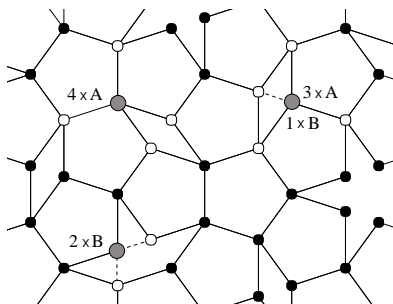


FIG. 5: The orientation of a decagon on a vertex in a PPT is fixed in the case of four A- or two B-neighbors (left). The only vertices with a choice for the decagon orientation are the obtuse rhombus corners, which have three A-neighbors and one B-neighbor (right).

To see this, we note that the orientation of a cluster on a vertex in a PPT is completely fixed by the presence of four A-neighbors or two B-neighbors (Figs. 5 and 6(a–d)), as in these cases the four A- or the two B-overlap zones, respectively, are completely saturated. A-neighbors are separated by an edge of a tile or a long diagonal across a ship or star, whereas B-neighbors are separated by a short diagonal of a rhombus, ship or star. The only vertices whose cluster orientation is not fixed by their local environment in the tiling are the obtuse corners of the rhombi, which have three A-neighbors and one B-neighbor (Figs. 5 and 6(e)). Therefore, two cluster orientations are possible for each obtuse rhombus corner. For the fully relaxed rule, where no orientation conditions for the overlaps have to be obeyed, we thus have altogether four choices per rhombus for the cluster orientations.

However, for the relaxed overlap rule we have to obey the orientation condition for the B-overlaps. It is easily shown that this condition is always satisfied for B-overlaps across ships and stars. In order to fulfill the orientation condition for B-overlaps across rhombi, too, the orientations of the clusters on opposite obtuse rhombus corners cannot be chosen independently. If for one of the corners an orientation is chosen, the orientation of the other is already fixed, i. e., the condition is satisfied only for two of the four possible combinations mentioned above.

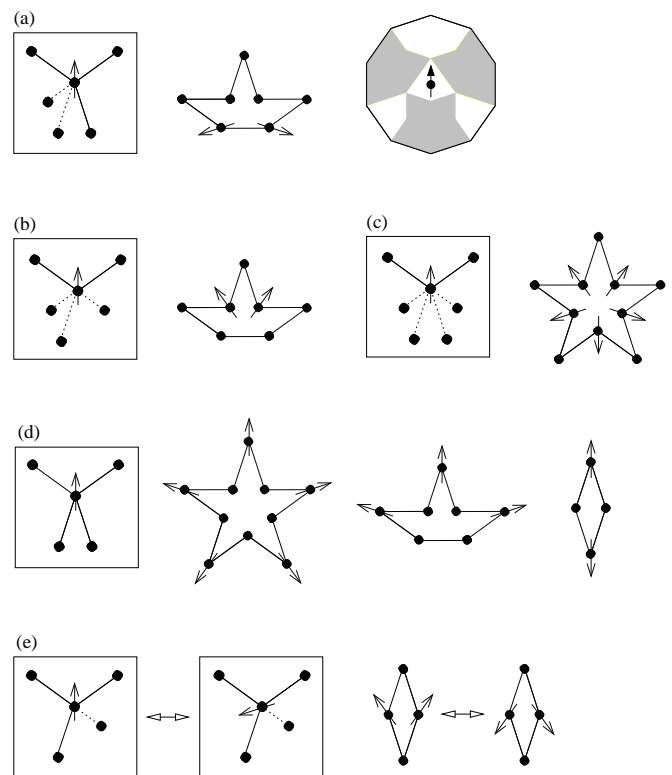


FIG. 6: Orientation of a decagon on a vertex in the PPT, depending on the local environment. The orientations are given by an arrow, as defined in the upper right corner.

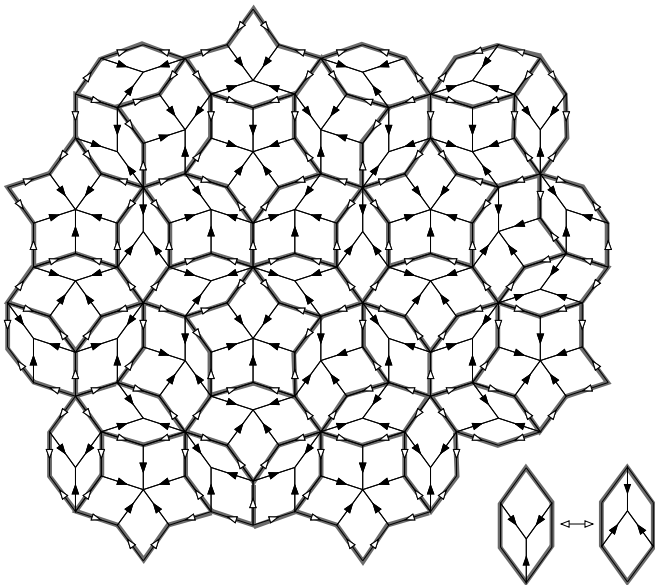


FIG. 7: Relationship between 4-level (thin black lines) and 2-level random tilings (thick gray lines). The matching rules for the “double” arrows (here drawn in black) are still obeyed. Since the matching rules for the “single” arrows (here drawn in white) are no longer maintained, each hexagon of the 2-level or random HBS tiling can be subdivided in two different ways, as shown in the bottom right corner.

In the same way, one can quantify the relationship between the cluster coverings and certain variants of random Penrose rhombus tilings. The random HBS tilings arise from random Penrose rhombus tilings still satisfying the matching rules for “double” arrows (drawn in black in Fig. 7). Such random Penrose rhombus tilings are also called 4-level random tilings.<sup>12,17</sup> When the edges with a double arrow are simply wiped out, we obtain the random HBS tilings, which are also known as 2-level tilings.<sup>12</sup> The relationship between 4-level and 2-level random tilings is not one-to-one: Whereas the subdivision of boats and stars is unique, there are two choices for the subdivision of each hexagon into rhombi (Fig. 7), just as there are two possible cluster assignments on the obtuse rhombus corners in the PPT, as discussed above (Fig. 6(e)). Since rhombi in the PPT and hexagons in the HBS tiling are in one-to-one correspondence (Fig. 4), this implies that the multiplicity of relaxed cluster coverings and 4-level random tilings, related to a given random PPT, is the same. Apart from the extra multiplicities, the relaxed covering rule is therefore equivalent to the Penrose double-arrow matching rules (ignoring single arrows), whereas the Gummelt covering rule is equivalent to the full Penrose matching rules.

### III. CLUSTER DENSITY MAXIMIZATION

In the last section, we have considered *cluster coverings*, where our clusters have simply been decagons with

certain overlap rules. Another variant of an ordering principle for quasicrystals based on a cluster picture is the *cluster density maximization*,<sup>3,5,8</sup> which we will consider in the following.

The relaxed overlap rule discussed above allows for a very natural realization in terms of a *vertex cluster* in the PPT. This vertex cluster is shown in Fig. 8. We have to point out that the tile edges are drawn only as a guide to the eye; they are not part of the cluster, only the vertex set counts. It is easy to see that the vertex set of the cluster cannot enforce the orientation of the small A-overlaps of the Gummelt decagon, whereas the orientation of the B-overlaps is intrinsically enforced. The A-overlap consists of a rhombus or a rhombic area inside a ship or star without orientation, and the B-overlap is formed essentially of a hexagon-shaped area with an interior vertex in asymmetric position which yields an orientation (Fig. 8).

With this cluster, we can build a statistical model for the cluster density maximization. We consider the set of all random PPTs (we still require that spiky tiles are completely surrounded by pentagons) and assign to each tiling a statistical weight which is simply the number of vertex clusters it contains. With a suitable MC algorithm, it is then possible to find the subensemble of those random PPTs which have maximal cluster density. For this purpose, we need a MC dynamics which is ergodic in the ensemble of all random PPTs. By repeated flips it is then possible to turn any random PPT into any other.

We have found (see Sec. IV) that the flip moves shown in Fig. 9 have the required properties. The flip configurations consist of a hexagon with an interior vertex which can jump to its “mirror image”. This move corresponds to a change in the orientation of the hexagon by 180°. The vertices of the hexagon itself are not affected, but the adjacent tile configurations are changed depending on the local environment. In Fig. 9(a), e. g., the adjacent ship and rhombus are exchanged, or in Fig. 9(b), a star and a rhombus are transformed into two ships, etc. These flips preserve the property that the spiky tiles

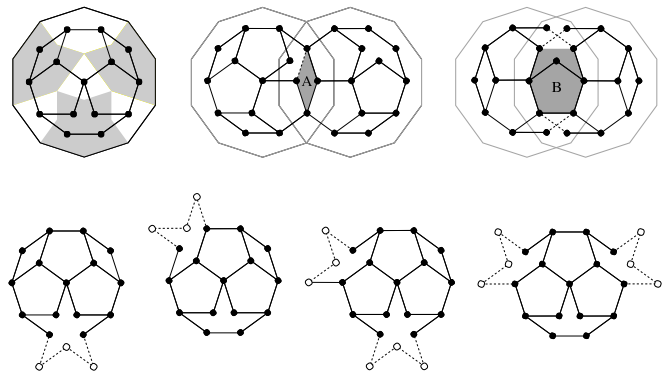


FIG. 8: Vertex cluster, superimposed on the Gummelt decagon (top left), and representative A- and B-overlaps (top middle and right). This cluster enforces the relaxed overlap rules. The bottom row shows examples of tile configurations for the vertex cluster.

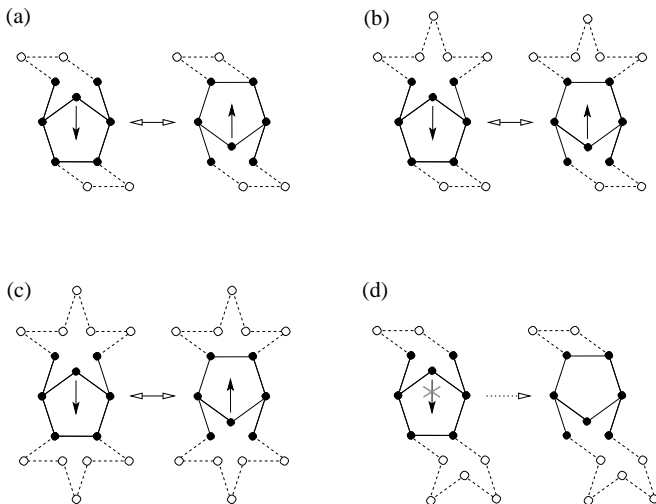


FIG. 9: Flip moves for the MC simulation. The flips (a–c) are allowed, whereas move (d) is forbidden since it would produce a new kind of tile (the zigzag-shaped configuration at the bottom).

are always surrounded by pentagons. There are some “flip configurations” where the local environment prohibits the flip. This is the case for configurations like in Fig. 9(d), where the flip would introduce a new kind of tile (see also Ref. 18). In all our simulations, such flips were forbidden. For the sake of completeness, it is explicitly shown in Fig. 10 how a new cluster can be created by a single flip.

The flips used for the PPT are in direct correspondence with hexagon flips in the associated 4-level Penrose tiling. This is illustrated in Fig. 11. Note that the other type of hexagon flip plays no role, because it leaves the HBS tiling, and thus the PPT invariant. As it is known that hexagon flips are ergodic for the 4-level Penrose tiling, this correspondence adds further confidence that the PPT flips are indeed ergodic, too.

With this MC scheme, the states of maximal cluster density can be determined by simulated annealing, using as energy the negative of the number of clusters, thus mimicking the total cohesion energy of the clusters. Then the energetic ground state, reached at low temperatures, is the ensemble of states with maximal cluster density. The method we use is based on the Metropolis impor-

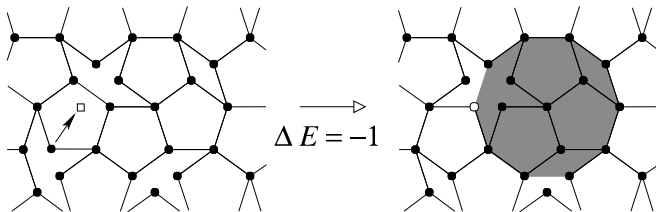


FIG. 10: Creation of a new cluster by a single flip, which lowers the total energy.

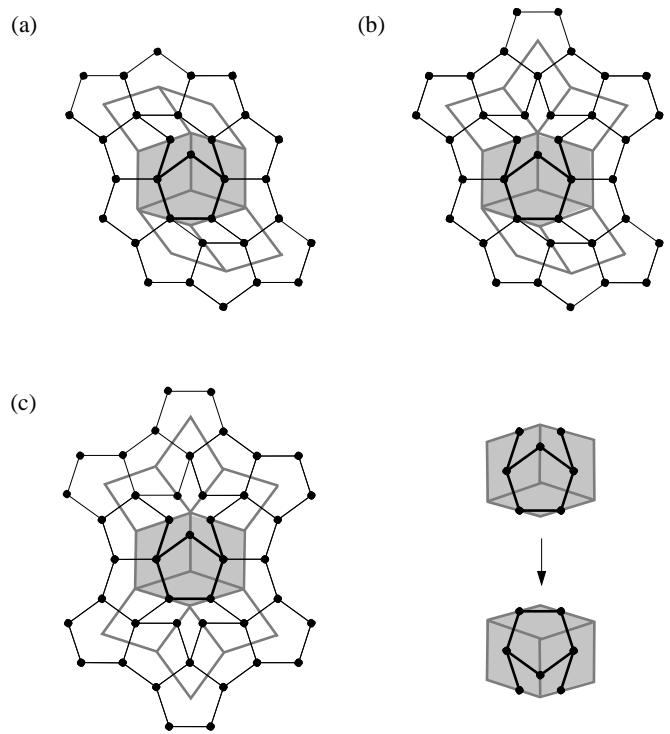


FIG. 11: Relationship between the flip configurations in the PPT (black), as shown in Fig. 9, and the corresponding local tile configurations in the random Penrose rhombus tiling (gray), which were used in Ref. 17. The flip move is explicitly shown in the bottom right corner.

tance sampling algorithm.<sup>17,19</sup> The basic MC move is as follows: (i) Choose a vertex randomly. (ii) If it can be flipped, calculate the energy change  $\Delta E$  (which is the negative of the change in the number of clusters) and flip it with probability

$$p = \begin{cases} e^{-\beta\Delta E} & \text{for } \Delta E > 0, \\ 1 & \text{otherwise.} \end{cases} \quad (1)$$

This algorithm fulfills the condition of detailed balance.

It turns out that the states of maximal cluster density are *supertile random PPTs*, whose tiles have an edge length  $\tau^2$  times that of the small tiles (where  $\tau = (1 + \sqrt{5})/2$  is the golden number). An example of such a supertiling is shown in Fig. 12. It cannot be a perfect tiling, since it is still possible to move clusters in the ground state without changing their number. This is due to the fact that the relaxed rule and hence our vertex cluster does not enforce the orientation of the A-overlaps.

In view of the results of the previous section, this is of course not too surprising. The cluster centers sit on the vertices of the supertiling, covering all vertices of the small tiles. Since the vertex cluster is smaller than the Gummelt decagon, it does not cover the whole area, but only the vertices; there remain small pentagons uncovered, which sit at the center of the supertile pentagons. This does not affect the overlap constraints, however.

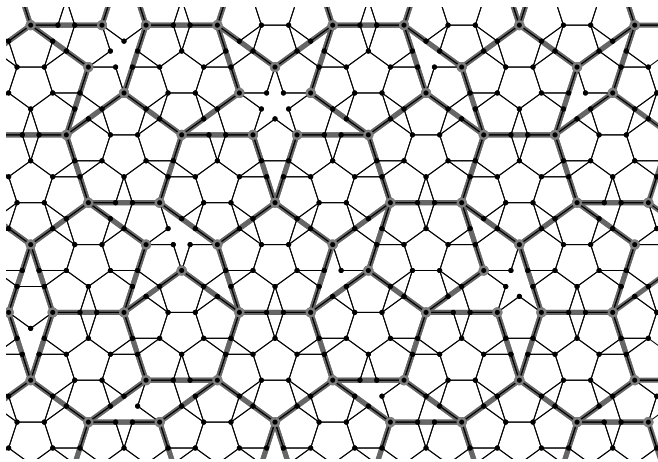


FIG. 12: Structure with maximal cluster density. The cluster centers form the vertices of a supertile random PPT (gray lines).

Our results therefore imply that there is a one-to-one correspondence between *decagon coverings satisfying the relaxed rule* and structures with *maximal density of the vertex cluster* (Figs. 3 and 12, respectively). Although these two ordering principles are very similar, they are conceptually slightly different and have to be distinguished.

Supertile random tiling ensembles as a result of cluster maximization were found already in Ref. 8. Maximizing star decagon clusters in a rhombus tiling leads to an ensemble of HBS-type supertile tilings.<sup>8,9</sup> That ensemble contains also other structures, however, which is not the case for our cluster. In particular, it should be noted that if the tile stoichiometry of the pentagons and spiky tiles admits an HBS supertile tiling, then the state of maximal cluster density is always an HBS supertile tiling. A phase separation as discussed in Ref. 9 is not possible. The only tiles that could be separated are the thin rhombi, but if there are enough pentagons, it is always advantageous to surround the rhombi with pentagons. The ensemble obtained by maximizing our vertex cluster is therefore a strict subensemble of the one obtained by maximizing the star decagon in random rhombus tilings.<sup>9</sup>

#### IV. ENTROPY DENSITY

With our cluster model, it is also possible to measure the entropy density of the ensemble of structures with maximal cluster density and thus the entropy density of the *relaxed cluster covering ensemble*. In the previous section, we have introduced an energy model which assigns a cohesion energy to each cluster in the structure. In this model, the ground state, i. e., the state of maximal cluster density, consists of supertile random PPTs with an extra weight of two per rhombus, because for each rhombus there are two choices of a cluster configuration with the same number of clusters, as shown in

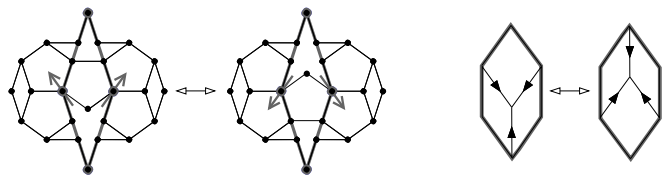


FIG. 13: In the supertile random PPT, each rhombus is counted twice because of the two possible cluster orientations on the obtuse corners (left). This is in one-to-one correspondence with the hexagons in the 4-level random tiling (right).

Fig. 13 (see also Fig. 6(e)). At infinite temperature, on the other hand, we have the full random PPT (at the level of the small tiles), where each rhombus is counted only once.

With the entropic sampling algorithm,<sup>19,20</sup> we can determine the entropy of the system as a function of energy. In this method, the Boltzmann probability  $e^{-\beta E}$  of the Metropolis algorithm is replaced by the factor  $e^{-S(E)}$ , where  $S(E)$  is the microcanonical entropy function. Since this factor is just the inverse of the number  $g(E)$  of states with energy  $E$ , according to

$$S(E) = \ln g(E) \quad (2)$$

(in units of  $k_B$ ), we obtain a uniform energy distribution

$$P(E) \propto g(E)e^{-S(E)} \equiv 1, \quad (3)$$

which corresponds to a random walk through the energy space of the system.

However, the exact entropy function  $S(E)$  is not known a priori, hence it has to be determined iteratively, starting with a rough estimate of  $S(E)$ . This estimate can be obtained by a short run using as “entropy function”  $S(E) \equiv 0$ , which yields an estimate for the degeneracy  $g(E)$  of the different energies and thus, via Eq. (2), an estimate for the real entropy function. Another possibility to get a good estimate is to take advantage of the extensive nature of entropy by scaling the entropy function of a smaller system to a larger one.

Subsequently, the entropy function is optimized by an iterative procedure. Analogously to the Metropolis algorithm, we choose for the flip probabilities

$$p = \begin{cases} e^{-\Delta S} & \text{for } \Delta S > 0, \\ 1 & \text{otherwise,} \end{cases} \quad (4)$$

where  $\Delta S = S(E + \Delta E) - S(E)$  is the change in entropy due to the considered MC move (with energy change  $\Delta E$ ). This choice of  $p$  likewise fulfills the condition of detailed balance. The iteration scheme is then as follows: (i) Run a MC simulation based on Eq. (4) in order to obtain an energy histogram  $H(E)$ . (ii) Use the measured histogram to correct the entropy function according to the update rule

$$S(E) \leftarrow \begin{cases} S(E) + \ln H(E) & \text{for } H(E) \neq 0, \\ S(E) & \text{for } H(E) = 0. \end{cases} \quad (5)$$

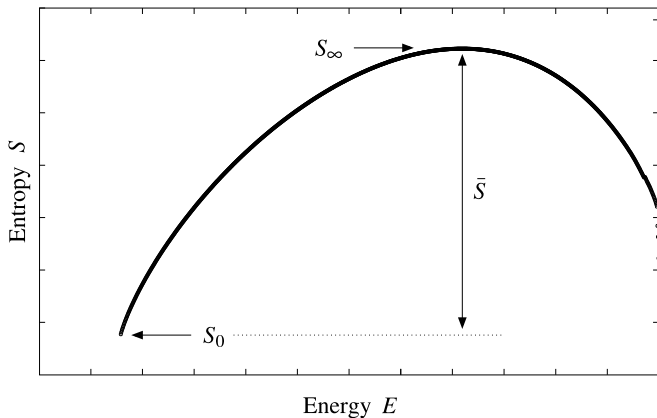


FIG. 14: Representative example of the microcanonical entropy as a function of the energy of the system.

(iii) Continue at (i) until the energy histogram is sufficiently uniform.

An example of such an entropy function is shown in Fig. 14. As this method does not yield absolute entropy values, we can only measure entropy differences, in particular the difference  $\bar{S}$  between the ground state and the infinite-temperature state (i. e., the maximum of the entropy function). The entropies at zero ( $S_0$ ) and infinite temperature ( $S_\infty$ ) are both entropies of random PPTs, once with a twofold degeneracy for each rhombus (Fig. 13), and once without. To compare these two entropy values, the latter one has to be corrected by adding an extra double-counting of the rhombi, which yields for each rhombus a factor of 2 in the degeneracy  $g_\infty$  or an additive contribution of  $\ln 2$  in the entropy  $S_\infty$ , respectively. Moreover, the two random tilings are at different length scales, since the supertile edges are  $\tau^2$  times larger than the small tile edges, which has to be taken into account due to the extensive nature of entropy. Therefore, we have the following relation between the two entropy densities  $\sigma_0$  and  $\sigma_\infty$ :

$$\tau^4 \sigma_0 = \sigma_\infty + \rho_{\text{rh}} \ln 2, \quad (6)$$

where  $\rho_{\text{rh}}$  is the measured rhombus density in the infinite-temperature state. If we write  $\sigma_\infty = \sigma_0 + \bar{\sigma}$ , we end up with an equation for the ground state entropy density  $\sigma_0$ , in which all other quantities can be measured:

$$\sigma_0 = \frac{1}{\tau^4 - 1} (\bar{\sigma} + \rho_{\text{rh}} \ln 2). \quad (7)$$

The ground state entropy density has been determined in this way for several periodic approximants. By finite-size scaling, the values can then be extrapolated to infinite system size. For this purpose, the entropy density, as a function of system size  $N$ , is fitted to a function of the (empirical) form  $a + be^{-c/N}$ , which proves to work very well (Fig. 15). At a scale where the supertile edges (which separate A-overlap neighbors in the cluster model) have unit length, we obtain a value of

$$\sigma_0/k_B = 0.253 \pm 0.001 \quad (8)$$

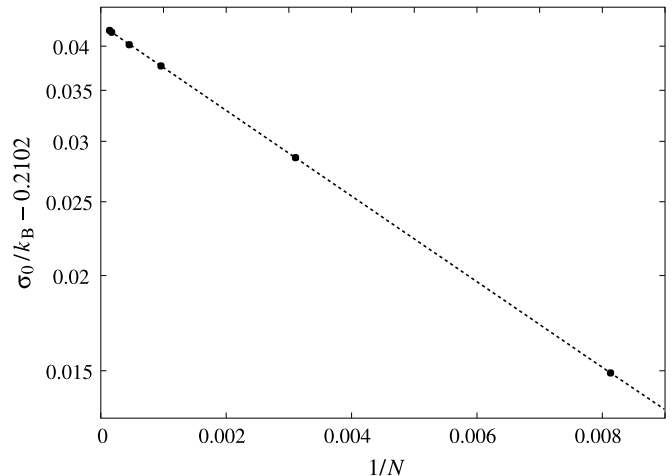


FIG. 15: Finite-size scaling of the entropy density of the relaxed cluster coverings, where  $N$  is the number of vertices. The applied fit function is of the (empirical) form  $\sigma(N) = a + be^{-c/N}$ . In this graph, the line  $\log[\sigma(N) - a] = \log b - c/N$  is shown. The error bars are smaller than the plot symbols.

for the *entropy density of the relaxed coverings*. This can be compared with the value which Tang and Jarić have obtained by Metropolis-type MC simulations for the entropy density of the 4-level random tiling.<sup>17</sup> In Sec. II, we have seen that 4-level random tilings are in one-to-one correspondence with relaxed cluster coverings (see also Fig. 13). If the different length scales of the two tilings are taken into account by a simple geometric conversion, the value of Tang and Jarić turns into

$$\sigma_0/k_B = 0.255 \pm 0.001, \quad (9)$$

which is compatible with our result.

## V. COUPLING BETWEEN CLUSTERS

The only difference between the *perfect* and the *relaxed* overlap rule is that the latter does *not* require *oriented* A-overlaps (whereas the orientation of the B-overlaps has to be obeyed). Since not all relaxed coverings are perfect, there must be A-overlaps which do *not* obey the orientation condition of the perfect rule. A closer analysis shows<sup>15,16</sup> that there is actually only one kind of disoriented A-overlap. All A-overlaps which can occur in relaxed coverings or supertile random PPTs, respectively, are shown in Fig. 16. For the disoriented A-overlap not permitted by the perfect rule (Fig. 16(d)), the two clusters have antiparallel orientations.

To order the (supertile) random tiling structures to perfect tilings, we introduce a coupling between neighboring clusters in such a way that overlaps which are not permitted by the perfect rule are energetically penalized. We expect such a coupling to be weak, because these kinds of defects can be detected only at larger scales. However, at low temperatures this coupling might still

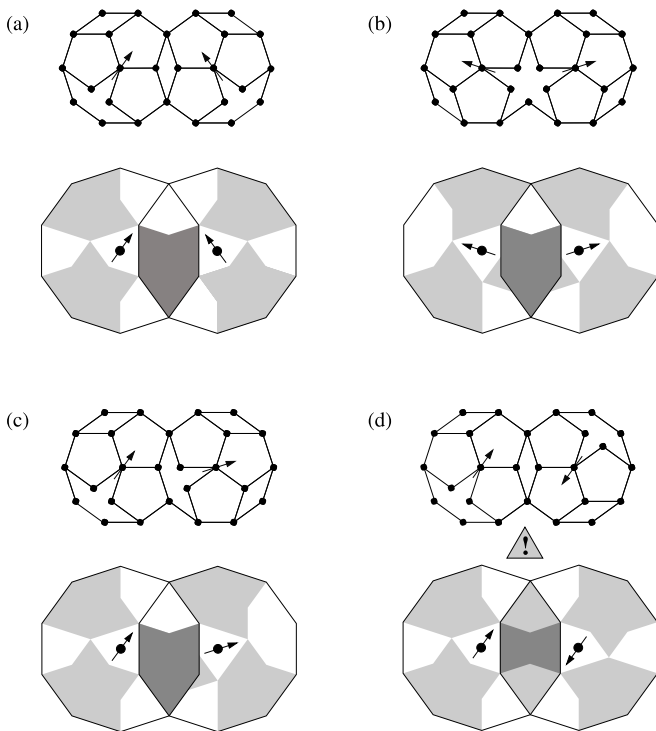


FIG. 16: Possible A-overlaps in supertile random PPTs or relaxed coverings. (a–c) obey the perfect rule. Only (d) is a disoriented overlap.

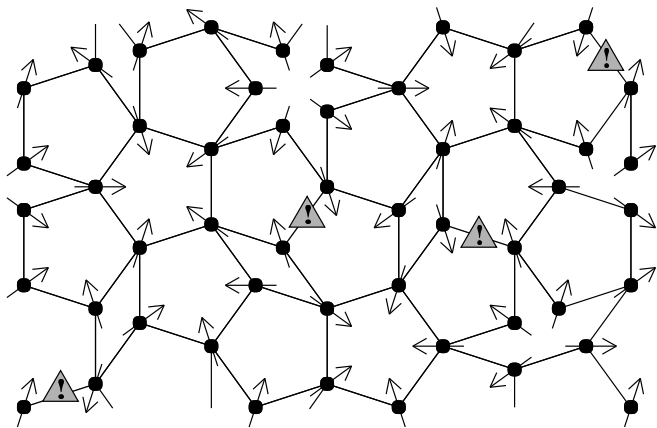


FIG. 17: Supertiling with cluster orientations indicated by arrows. The forbidden A-overlaps, corresponding to tile edges with antiparallel arrows at their ends, are marked.

be able to order the supertile random tiling ground state of the relaxed cluster covering to a perfectly quasiperiodic structure.

This suggests a scenario with two energy or temperature scales. The presence of each vertex cluster lowers the cohesion energy by a large amount, so that structures with maximal cluster density are strongly favored, even at relatively high temperatures. The equilibrium structures at these temperatures are therefore relaxed cluster coverings. Additionally, there is a small coupling between

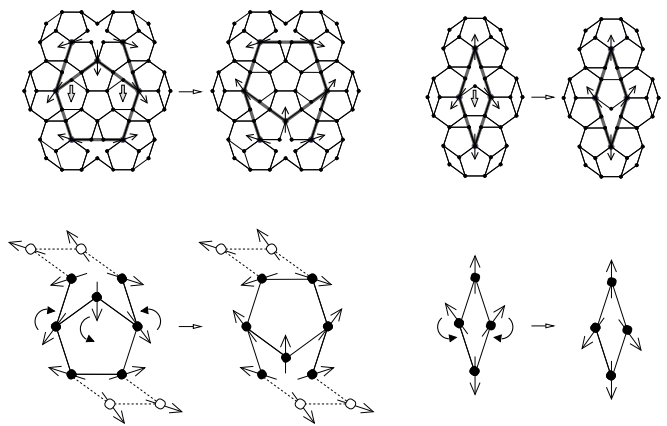


FIG. 18: Basic flips in the underlying tiling (top) and effective moves on the level of the supertiling (bottom). The hexagon flip (left) is the same as the one used before. Additionally, we also have the rhombus flip (right) which does not change the vertex structure of the supertiling. For both flip types, the cluster orientations have to be adjusted consistently with the underlying structure.

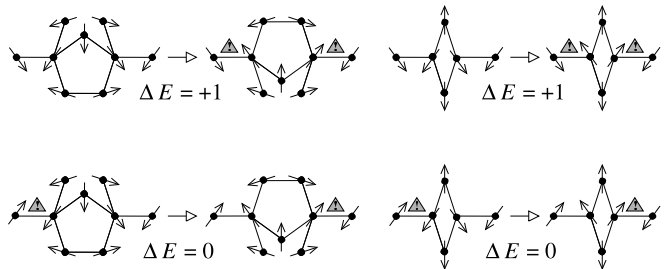


FIG. 19: Creation (top) and shift of defects (bottom) by single flips of the two types: hexagon flip (left) and rhombus flip (right).

neighboring clusters, which can order the supertile random tiling to a perfect tiling at low temperatures.

We have verified the feasibility of this approach by MC simulations. For this purpose, we consider only the subensemble of states with maximal cluster density. In other words: We run our simulations at the level of the supertiling. If we represent a cluster in the supertile PPT by its center and its orientation (given by an arrow), we can describe the covering in a much more compact way, as shown in Fig. 17. Such a setup keeps the number of clusters constant, so that we cannot leave the states of maximal cluster density, which simplifies the simulation considerably.

As flip moves we can still use those of Fig. 9, except that we now have to adjust the cluster orientations of several vertices in the flip configuration. We have to do this in a way consistent with the vertex configuration in the underlying tiling, which actually determines the cluster orientations (Fig. 18). The first type of flip consists of two simultaneous flips in the underlying tiling. We have to point out that for a hexagon-type flip configuration

like the one in Fig. 18 (bottom left) the cluster orientations on the obtuse corners of the adjacent rhombus have to be as shown. Otherwise, the flip is not allowed, since then the cluster orientations would be inconsistent with the ship-shaped vertex configuration after the flip.

Additionally, we have to introduce a new type of flip which only changes the cluster orientations on the obtuse corners of a rhombus, but keeps the tiling itself fixed. Such a move corresponds to a single flip in the underlying tiling. In comparison with the flip moves in a Penrose rhombus tiling,<sup>12,17</sup> the hexagon flip corresponds to D-type and the rhombus flip to Q-type configurations.<sup>21</sup>

This MC dynamics can change the number of defects, as demonstrated in Fig. 19. Again, we have used a Metropolis-type MC scheme,<sup>17,19</sup> now with the number of defects as energy. We have seen in our simulations that the coupling of the clusters, which penalizes the defects, is indeed capable of ordering the random tilings to perfectly quasiperiodic structures. In other words: The ground state, reached by simulated annealing, is a perfect PPT, whereas the high-temperature state is a supertile random tiling or relaxed cluster covering. In this respect, “high” temperature means high compared to the cluster coupling, but still low compared to the energy required to break up clusters.

We have to mention that the ground state is not always a perfect PPT. Perfectness is determined by lifting the vertices to hyper-space; if the projections of the vertices onto the perpendicular space are all inside the acceptance region, the tiling is perfect, otherwise it is not. Since we use periodic approximants of PPTs in our simulations, the minimal number of defects is always larger than zero.<sup>22</sup> These defects can be shifted without changing the energy. In this process, a vertex can leave the acceptance region in the perpendicular space. Thus, the tilings with minimal number of defects are not necessarily perfect.

With the model of coupled clusters, it is also possible to measure the entropy density of the relaxed covering ensemble. In this case, the ground state is ordered and has zero entropy (at least in the thermodynamic limit), and the high-temperature state is the one whose entropy we are interested in. We therefore only need to measure the difference between the entropies of the high-temperature state and the ground state, and extrapolate these values to infinite system size. It turns out, however, that the finite-size scaling for this model does not work as well as for the model with a supertile random tiling in the ground state as considered in Sec. IV. The results are therefore less precise, but nevertheless consistent.

## VI. DISCUSSION AND CONCLUSION

In this paper, we have discussed different ordering principles for quasicrystals based on the cluster picture, namely the cluster covering principle and the principle of cluster density maximization. A relaxed version of the

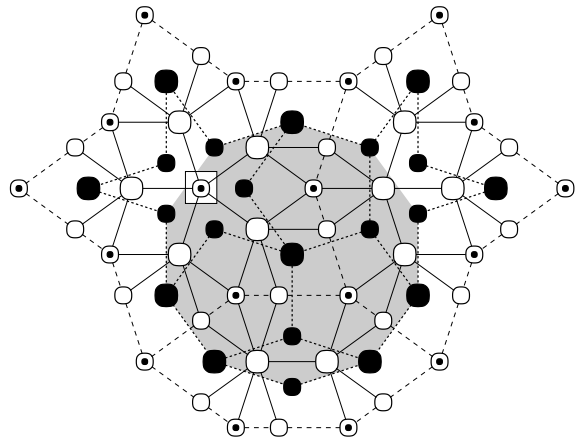


FIG. 20: Atomic cluster found by Roth and Henley<sup>23</sup> in a molecular dynamics simulation. White atoms are at  $z = 0$ , black atoms at  $z = \frac{1}{2}$ , and dotted atoms at  $z = \frac{1}{4}, \frac{3}{4}$  (in units of the period in  $z$ -direction). The area of our vertex cluster is shaded in gray. At the center of a star (marked with a box), we would have expected a different atomic configuration (see text).

covering rules for Gummelt’s aperiodic decagon has been considered, which produces as ground state a supertile random PPT. It has been shown that this relaxed overlap rule has a very natural realization in terms of a vertex cluster in the PPT.

The feasibility of our model has been tested by MC simulations. In particular, we have verified that the relaxed cluster coverings coincide with the states of maximal cluster density. The entropy density measured in the random covering ensemble is found to agree with the entropy density obtained by Tang and Jarić for the equivalent random 4-level tiling. Moreover, we have shown that a coupling between neighboring clusters can order the random-tiling-type ground states to a perfectly quasiperiodic structure.

Models of this kind can be very suitable for the explanation of experimentally observed decagonal quasicrystals, as the latter are often not perfectly quasiperiodic, but more of a random tiling nature.<sup>16</sup> Random PPTs, and the closely related HBS tilings, are often observed in high-resolution electron microscopy images (Fig. 1, compare Figs. 3 and 12).<sup>1,2</sup>

The most striking resemblance, however, is with a three-dimensional atomic cluster found by Roth and Henley<sup>23</sup> in a molecular dynamics simulation of binary decagonal Frank-Kasper-type quasicrystals (Fig. 20), whose lateral overlap constraints are almost the same as those of our two-dimensional vertex cluster. The only discrepancy is at the center of a star, where for full equivalence we would have expected a single atom at  $z = 0$  in the Roth-Henley cluster, not two atoms at  $z = \frac{1}{4}, \frac{3}{4}$ .

The vertex set of our cluster can be realized by several tile configurations in the PPT (Fig. 8). This might possibly be related to the results of an Al-Co-Ni structure analysis by Cervellino, Haibach, and Steurer.<sup>24</sup> They ob-

served that there is a perfectly quasiperiodic long-range order of the centers of atomic clusters, but the interior structure of the clusters themselves is disordered. This means that the local atomic interactions cannot enforce local order, but there exists a long-range order. The proposed mechanism for long-range ordering is the electronic long-range term of free electrons. These long-wavelength electrons “see” only a simpler, “smeared out” version of the complex cluster structure.

As we have seen in Sec. V, the shift of a flipping cluster center is large, whereas the corresponding two vertex moves in the underlying tiling are small (Fig. 18). In the atomic simulations of Al-Co-Ni done by Honal and Wellberry,<sup>18</sup> the flip of a cluster corresponds to jumps of only four atoms. The magnitude of these jumps is small (about 1 Å) compared to the scale of the clusters (about 20 Å).

All our simulations have been in two dimensions. It is well known that, for finite-range interactions, quasicrystal structures in two dimensions cannot be stable at any positive temperature.<sup>25</sup> At non-zero temperatures, they

are always in a random tiling state, the “phase transition” from the ordered phase to the random tiling state being at zero temperature. However, in three dimensions the critical temperature is expected to be positive. For this purpose, one can consider as three-dimensional system a stacking of our two-dimensional models with a suitable coupling between neighboring layers. Such layered *tiling* models have already been studied by Jeong and Steinhardt,<sup>26</sup> but are possible also in the *cluster covering* setting. As expected for three-dimensional systems, the phase transition from ordered to random-tiling-type structures is at finite temperature. The results of these studies will be presented in a separate paper.<sup>27</sup>

### Acknowledgments

We would like to thank Petra Gummelt for useful discussions on the relationships between the different relaxed coverings and random tiling ensembles.

- 
- \* Present address: Fachbereich Physik, Universität Konstanz, D-78457 Konstanz, Germany; Electronic address: michael.reichert@uni-konstanz.de
- <sup>1</sup> S. Ritsch, C. Beeli, H.-U. Nissen, T. Gödecke, M. Scheffer, and R. Lück, *Phil. Mag. Lett.* **74**, 99 (1996).
  - <sup>2</sup> C. Soltmann and C. Beeli, *Phil. Mag. Lett.* **81**, 877 (2001).
  - <sup>3</sup> F. Gähler, *Mat. Sci. Eng. A* **294–296**, 199 (2000).
  - <sup>4</sup> P. Gummelt, *Geometriae Dedicata* **62**, 1 (1996).
  - <sup>5</sup> H.-C. Jeong and P. J. Steinhardt, *Phys. Rev. B* **55**, 3520 (1997).
  - <sup>6</sup> S. I. Ben-Abraham and F. Gähler, *Phys. Rev. B* **60**, 860 (1999).
  - <sup>7</sup> F. Gähler, R. Lück, S. I. Ben-Abraham, and P. Gummelt, *Ferroelectrics* **250**, 335 (2001).
  - <sup>8</sup> H.-C. Jeong and P. J. Steinhardt, *Phys. Rev. Lett.* **73**, 1943 (1994).
  - <sup>9</sup> C. L. Henley, in *Proceedings of the 6th International Conference on Quasicrystals*, edited by S. Takeuchi and T. Fujiwara (World Scientific, Singapore, 1998), p. 27.
  - <sup>10</sup> F. Gähler, *Phys. Rev. Lett.* **74**, 334 (1995).
  - <sup>11</sup> Y. Yan and S. J. Pennycook, *Phys. Rev. Lett.* **86**, 1542 (2001).
  - <sup>12</sup> C. L. Henley, in *Quasicrystals: The State of the Art*, edited by D. P. DiVincenzo and P. J. Steinhardt (World Scientific, Singapore, 1991), p. 429.
  - <sup>13</sup> E. Abe, K. Saitoh, H. Takakura, A. P. Tsai, P. J. Steinhardt, and H.-C. Jeong, *Phys. Rev. Lett.* **84**, 4609 (2000).
  - <sup>14</sup> A brief overview of this work has been published in: F. Gähler and M. Reichert, *J. Alloys Comp.* **342**, 180 (2002).
  - <sup>15</sup> P. Gummelt and C. Bandt, *Mat. Sci. Eng. A* **294–296**, 250 (2000).
  - <sup>16</sup> P. Gummelt, *Combination of Cluster Covering Approach and Random Tiling Model* (preprint, 2002).
  - <sup>17</sup> L.-H. Tang and M. V. Jarić, *Phys. Rev. B* **41**, 4524 (1990).
  - <sup>18</sup> M. Honal and T. R. Welberry, *Z. Kristallogr.* **217**, 109 (2002).
  - <sup>19</sup> For a detailed survey of Monte Carlo methods, see, e. g.: M. E. J. Newman and G. T. Barkema, *Monte Carlo Methods in Statistical Physics* (Oxford University Press, New York, 1999).
  - <sup>20</sup> J. Lee, *Phys. Rev. Lett.* **71**, 211 (1993).
  - <sup>21</sup> N. G. de Bruijn, *Nederl. Akad. Wetensch. Proc. Ser. A* **84**, 53 (1981).
  - <sup>22</sup> O. Entin-Wohlman, M. Kléman, and A. Pavlovitch, *J. Phys. France* **49**, 587 (1988).
  - <sup>23</sup> J. Roth and C. L. Henley, *Phil. Mag. A* **75**, 861 (1997).
  - <sup>24</sup> A. Cervellino, T. Haibach, and W. Steurer, *Acta Cryst. B* **58**, 8 (2002).
  - <sup>25</sup> P. A. Kalugin, *JETP Lett.* **49**, 467 (1989).
  - <sup>26</sup> H.-C. Jeong and P. J. Steinhardt, *Phys. Rev. B* **48**, 9394 (1993).
  - <sup>27</sup> M. Reichert and F. Gähler, cond-mat/0302074 (2003).